Electronic Supplementary Material (ESI) for Nanoscale.

Supporting Information

Pt Alloy Nanoparticles Decorated on Large-Size Nitrogen-Doped Graphene Tubes for Highly Stable Oxygen-Reduction Catalysts

Mengjie Chen,[a,1] Sooyeon Hwang,[b,1] Jiazhan Li,[a] Stavros Karakalos,[c] Kate Chen,[a] Yanghua He,[a]

Shreya Mukherjee,[a] Dong Su,[b,*] and Gang Wu[a,*]

[a] Department of Chemical and Biological Engineering, University at Buffalo, The State

University of New York, Buffalo, New York 14260, United States

[b] Center for Functional Nanomaterials, Brookhaven National Laboratory, Upton, NY 11973, United States

[c] Department of Chemical Engineering, University of South Carolina, Columbia, SC 29208, United States

[1] These two authors contributed equally

Corresponding authors: dsu@bnl.gov (D Su); gangwu@buffalo.edu (G.Wu.)

Experimental details

Figures S1 to S19

Tables S1 to S2

Experimental Section

Synthesis of nitrogen-doped graphene tubes (NGTs)

The dicyandiamide (DCDA) was applied as a source of nitrogen and carbon. Metal acetates are crucial for the formation of graphene tubes because of the catalysis of transition metal nanoparticles. Three types of NGTs were synthesized by modifying the types of transition metals and their combination (e.g., Co, Ni, and CoNi). Typically, DCDA were dissolved in Millipore water under stirring at 60°C to form a transparent solution. Then the metal acetates were added in the solution. Specifically, the molar ratio among DCDA and metal salts was kept as 12:1. After 4-hour stirring at 60°C, the water was gradually evaporated at 70°C under stirring to obtain precipitation. While the precipitation was dry enough, the product was ball-milled uniformly to become powder. Then the nitrogen-doped graphene tubes were formed by performing one-step heat treatment at 1000°C for 3h under N_2. Afterwards, the NGTs were acid leached in 1M HCl at 60°C for 5h to remove the metal or metal oxides on the surface. In the end, the NGTs were washed with Millipore water for several times and dried at 60 °C in a vacuum oven for 12 hours. Three different graphene tubes are labeled as NGT(CoNi), NGT(Co), and NGT(Ni), respectively.

Synthesis of Pt supported on nitrogen-doped graphene tubes (Pt/NGTs)

The Pt nanoparticle deposition were performed through an ethylene glycol (EG) reduction method with a 20 wt% Pt mass loading on NGTs. Typically, the NGTs supports were dispersed in EG followed by sonicating for 1 hour to form a homogeneous complex suspension. Then, a certain amount of chloroplatinic acid solution which was prepared by dissolving chloroplatinic acid in ethylene glycol, was added into the complex suspension under sonicating for 20 minutes with N_2 bubbling. The complex suspension was refluxed for 3 hours at 130 °C under continuous stirring with N_2 bubbling. The catalysts were washed with Millipore water and dried at 70 °C in a vacuum oven for 12 hours. The as-prepared catalysts are identified as Pt/NGT. Herein, three types of NGTs were applied as support, which were identified as Pt/NGT(CoNi), Pt/NGT(Co), and Pt/NGT(Ni), respectively. As the post-treatment is important to catalyst in terms of activity and stability, the Pt/NGT were post heat-treated in N_2 at 800°C for 1 hour. The final catalysts were identified as post-Pt/NGT(CoNi), post-Pt/NGT(Co), and post-Pt/NGT(Ni), respectively.

Material characterization

The N_2 isothermal adsorption/desorption was recorded at 77K on a Micromeritics TriStar II. Samples were degassed at 150 °C for 4 h under vacuum prior to nitrogen physisorption measurements. The morphology of supports was studied using scanning electron microscopy (SEM) on a Hitachi SU 70 microscope at a working voltage of 5 kV. X-ray diffraction (XRD) characterization was performed on a Rigaku Ultima IV diffractometer with Cu Kα X-rays to present crystal phases in each sample. TEM images were obtained with JEOL JEM-2100F transmission electron microscope at an accelerating voltage of 200 kV at Brookhaven National Laboratory. Raman spectroscopy was performed using a Renishaw Raman system at 514 nm excitation. Samples were prepared as ink on a standard microscope glass slide, with the excitation laser focused through a 50× microscope objective for a total interrogation spot size of 1.0-micron diameter. Excitation power was held at 150 μW for all samples. X-ray photoelectron spectroscopy (XPS) were performed using a Kratos AXIS Ultra DLD XPS system equipped with a hemispherical energy analyzer and a monochromatic Al Kα source. The monochromatic Al Kα source was operated at 15 keV and 150 W; pass energy was fixed at 40 eV for the high resolution scans. All samples were prepared as pressed powders supported on a metal bar for the XPS measurements

Electrochemical measurements

All electrochemical measurements were conducted by using a CHI electrochemical workstation (CHI760b) coupled with a rotating-ring disk electrode (RRDE, Pine, AFMSRCE 3005) in a three-electrode cell. A rotating ring disk electrode (RRDE) covered by a thin film of the catalysts was used as the working electrode. Each catalyst powder (3 mg) was ultrasonically dispersed in a 0.6 mL mixture of isopropanol and Nafion® (5 wt.%) solution to produce an ink. Then the ink was drop-casted on the rotating ring disk electrode with a designed Pt loading of 60 $\mu g_{Pt}/cm^2$. Then the working electrode was dried at room temperature to form a thin-film electrode. The catalyst-coated disk working electrode was subjected to cyclic voltammetry (CV) in N_2-saturated 0.1 M $HClO_4$ at a scan rate of 50 mV/s to activate the catalysts. The electrocatalytic activity for ORR was tested by steady-state measurement using staircase voltammetry with a step of 0.05 V at intervals of 30 s from 0 to 1.1 V vs. RHE in O_2-saturated 0.1 M $HClO_4$ solution at 25 °C and a rotation rate of 900 rpm. The stability of catalyst was studied by potential cycling at 0.6 to 1.0 V (100 mV/s) in 0.1 M $HClO_4$ electrolyte at 25°C. For carbon corrosion test, accelerated stress tests via cyclic voltammetry were performed from 1.0 to 1.5 V (500 mV/s) at 25°C and 60°C. A graphite rod and an $Hg/HgSO_4$ (K_2SO_4-sat.) electrode were used as the counter and reference electrodes, respectively. The reference electrode was calibrated with respect to RHE by bubbling pure H_2 at 1.0 atm into a calibration tube fitted with a Pt wire coated with Pt black before each measurement.

Additional electrochemical and physical characterization

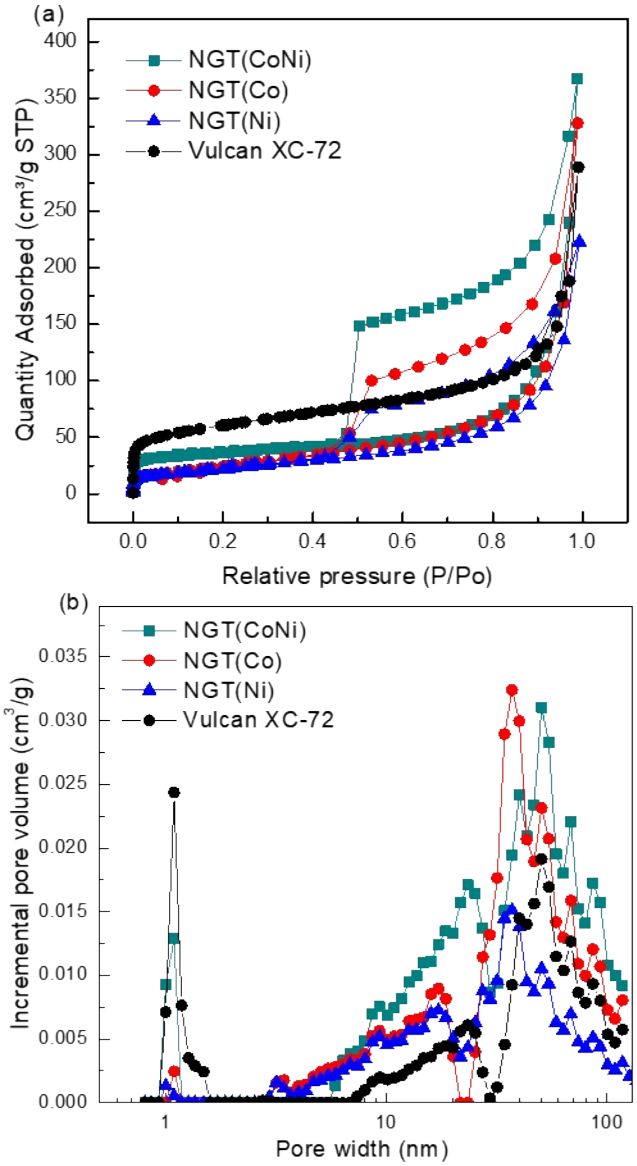

Figure S1. N_2 adsorption/desorption plots (a) and pore size distribution (b) of different carbon supports.

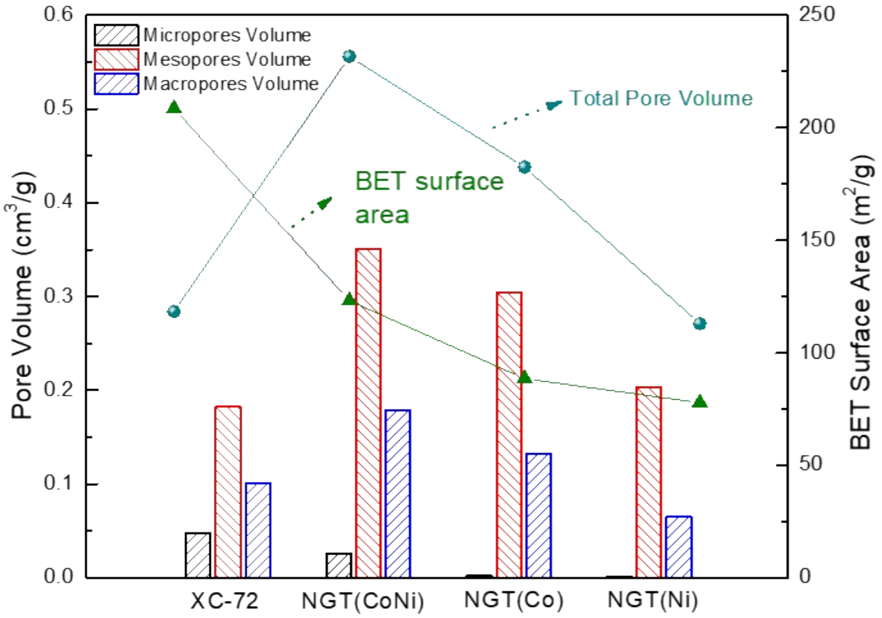

Figure S2. Comprehensive comparison of BET surface areas and porosity for various carbon supports.

Table S1. Pore size distribution and BET surface areas of different carbon support.

	V_{micro}		V_{meso}		V_{macro}		V_{total}	S_{BET}
Samples	$/cm^3g^{-1}$	%	$/cm^3g^{-1}$	%	$/cm^3g^{-1}$	%	$/cm^3g^{-1}$	$/m^2g^{-1}$
XC-72	0.048	16.9	0.183	47.5	0.101	35.6	0.284	208.5
NGT(CoNi)	0.026	4.7	0.351	63.1	0.179	32.2	0.556	123.1
NGT(Co)	0.00245	0.5	0.305	69.6	0.133	29.9	0.438	88.5
NGT(Ni)	0.00188	0.7	0.204	75.4	0.065	23.9	0.271	77.8

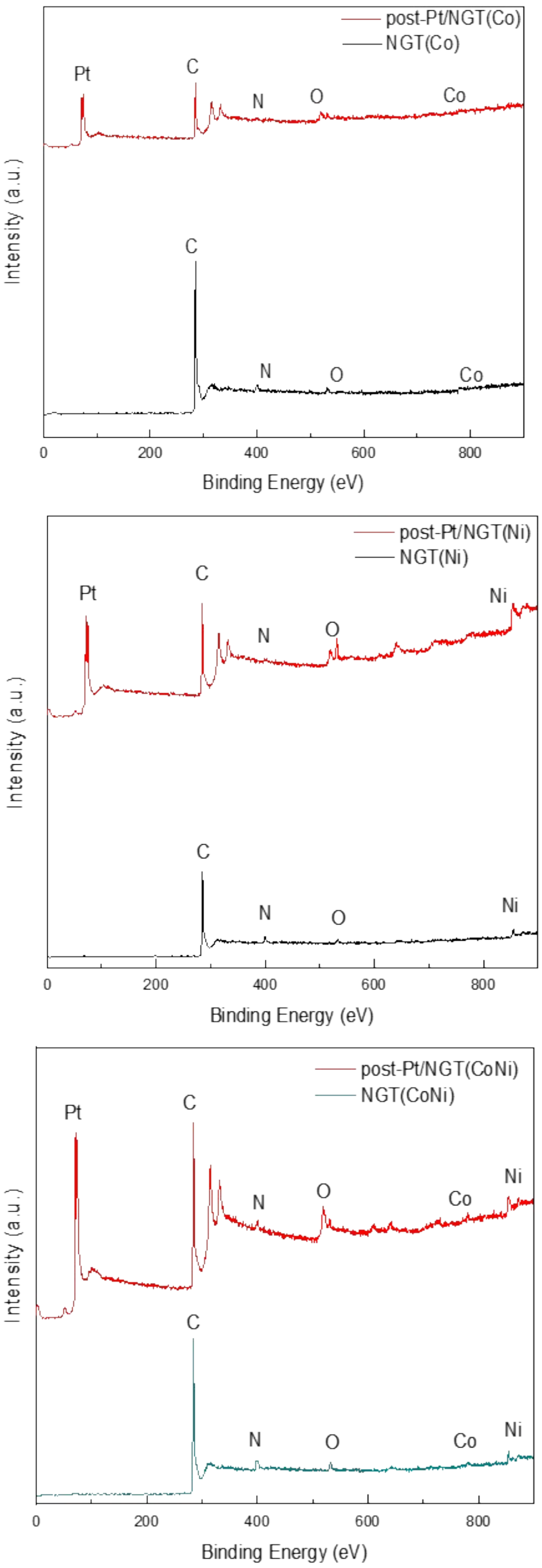

Figure S3. XPS survey spectra for different NGT supports and post-Pt/NGTs.

Table S2. XPS element quantification of supports and catalysts.

samples	Atomic concentration (%)					
	Pt	C	N	O	Co	Ni
NGT(CoNi)	0	95.2	2.6	1.7	0.1	0.4
NGT(Co)	0	97.3	1.5	1.1	0.1	0
NGT(Ni)	0	95.4	3.0	1.2	0	0.4
Pt/NGT(CoNi)	5.8	89.5	2.3	2.0	0.2	0.3
Pt/NGT(Co)	5.6	88.5	3.1	2.6	0.2	0
Pt/NGT(Ni)	8.0	86.1	2.8	2.8	0	0.3
post-Pt/NGT(CoNi)	4.8	90.6	2.4	1.6	0.2	0.4
post-Pt/NGT(Co)	3.6	92.4	2.0	1.8	0.2	0
post-Pt/NGT(Ni)	3.9	88.4	1.8	5.1	0	0.8

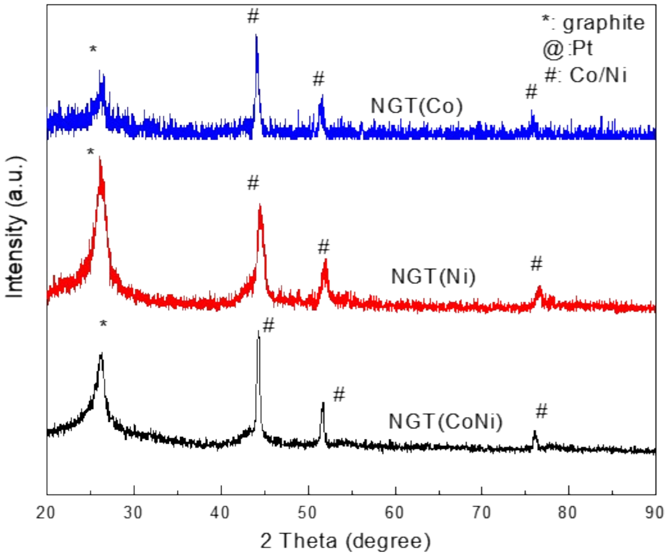

Figure S4. XRD patterns for various graphene tube supports.

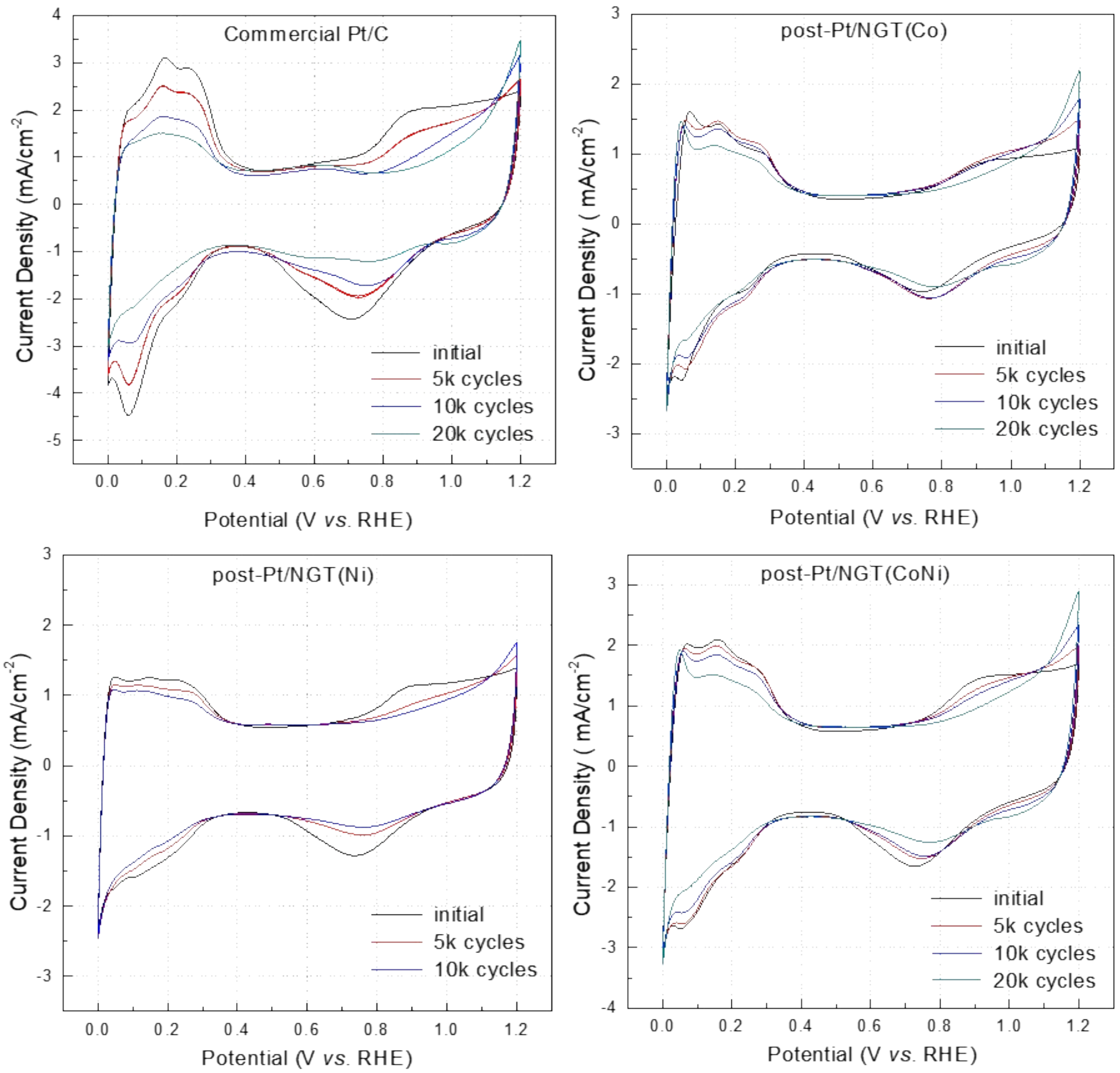

Figure S5. Cyclic voltammetry plots for different Pt cathode catalysts during ASTs. Potential cycling range from 0.6 to 1.0 V at a scan rate of 100 mV/s in 0.1 M $HClO_4$ at room temperature.

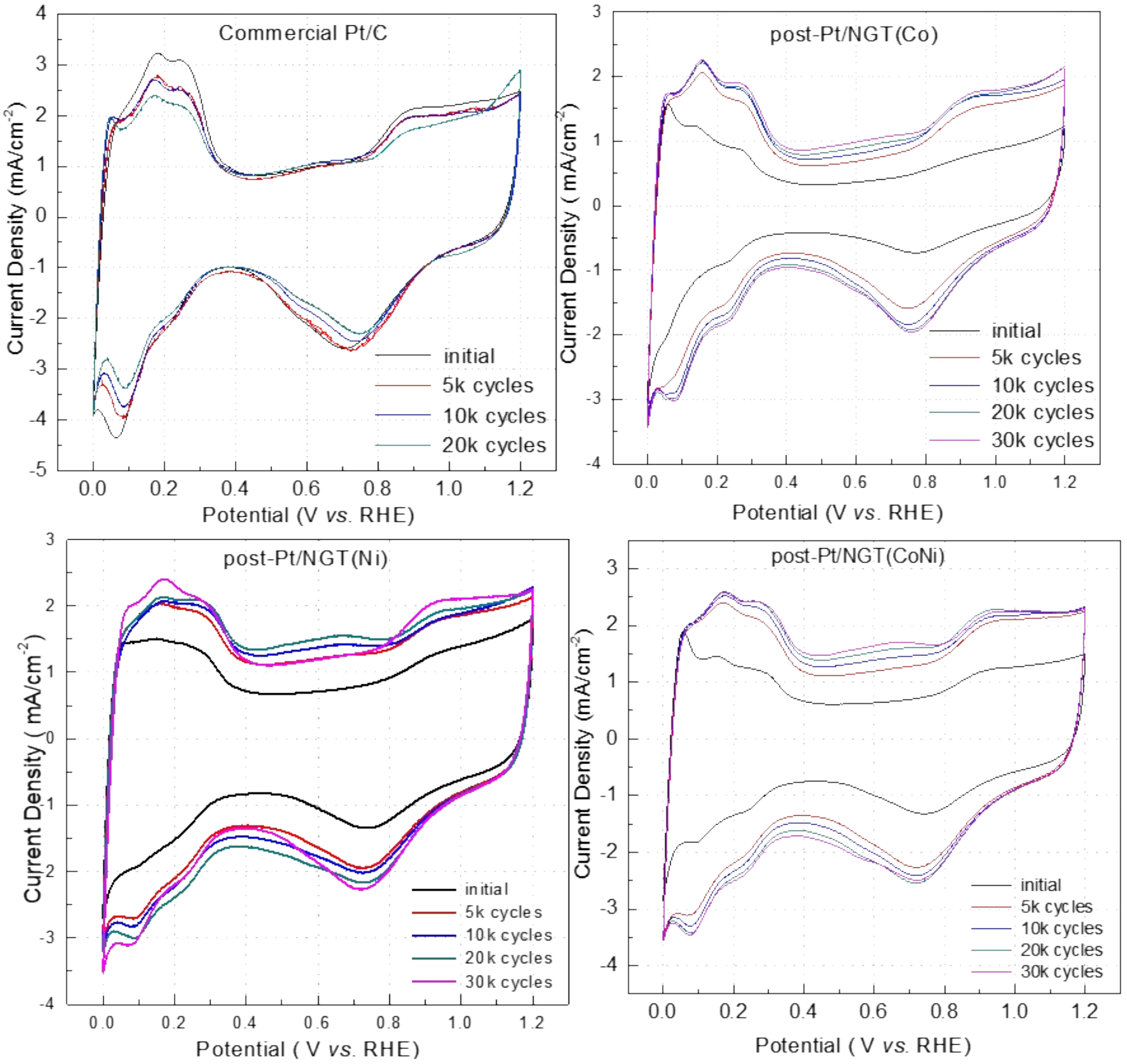

Figure S6. Cyclic voltammetry plots for different Pt cathode catalysts during ASTs. Potential cycling range from 1.0 to 1.5 V at a scan rate of 500 mV/s in 0.1 M $HClO_4$ at room temperature.

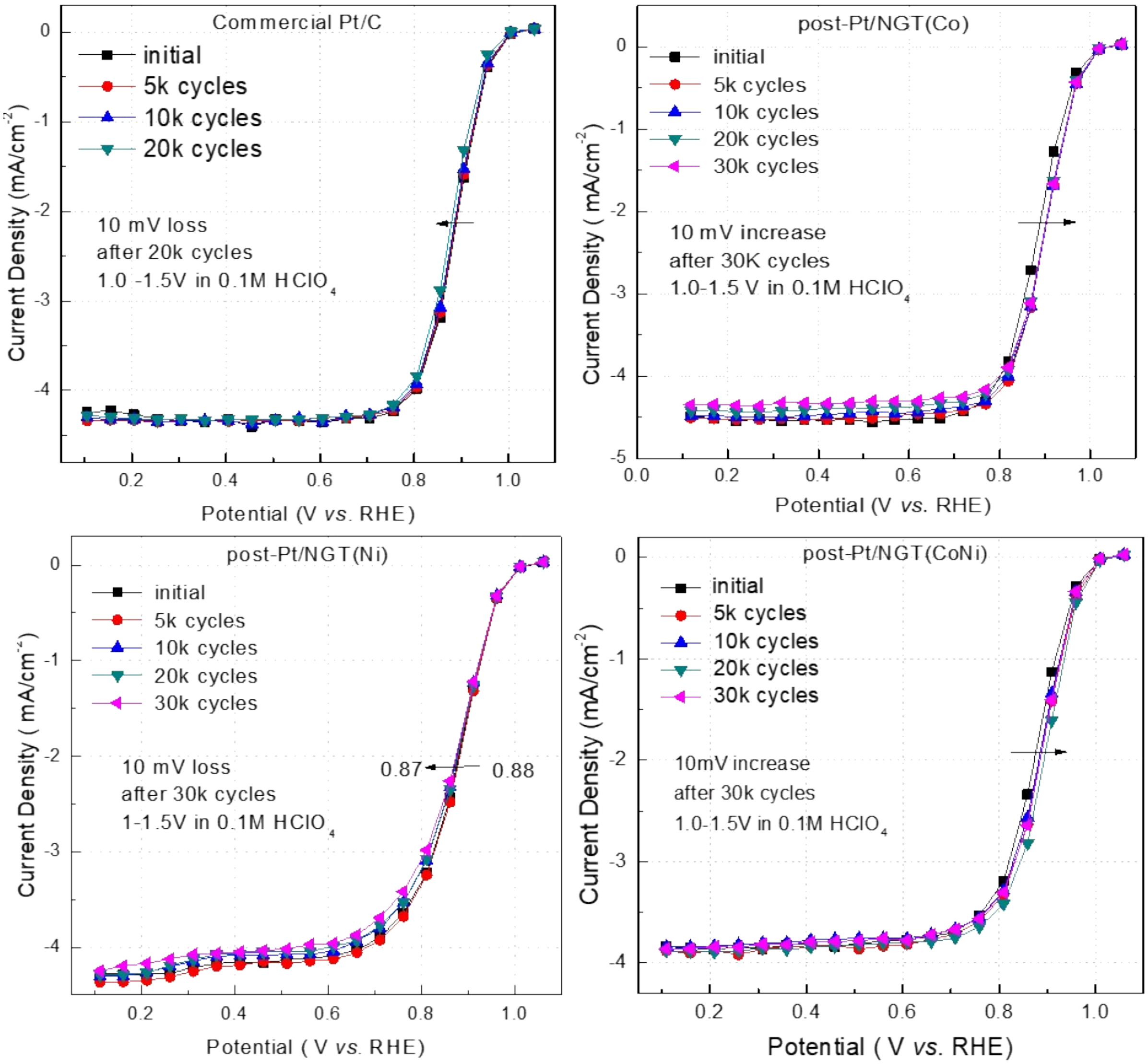

Figure S7. Steady-state polarization plots for different Pt cathode catalysts with rotation rate of 900 rpm during ASTs. Potential cycling range from 1.0 to 1.5 V at a scan rate of 500 mV/s in 0.1 M $HClO_4$ at room temperature.

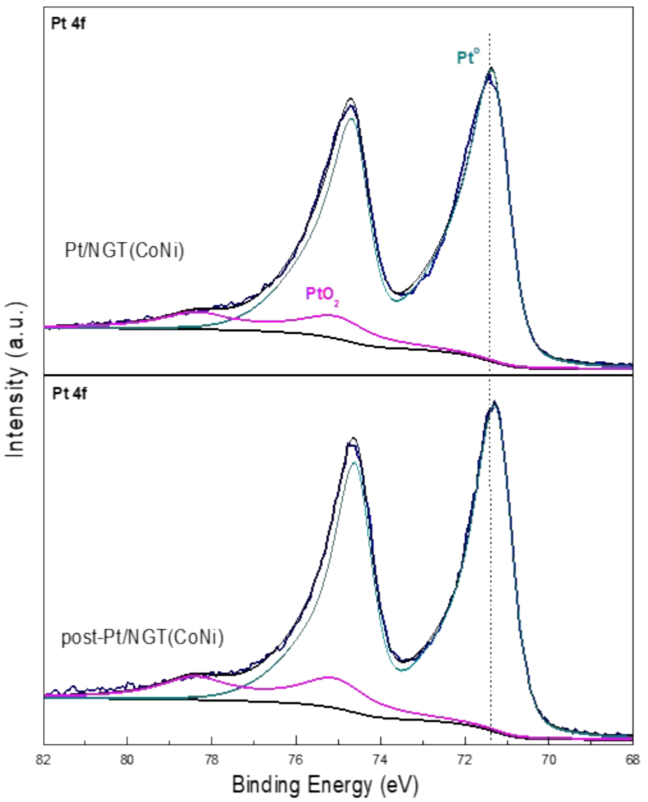

Figure S8. Pt 4f XPS spectra of Pt/NGT(CoNi) and post-Pt/NGT(CoNi).

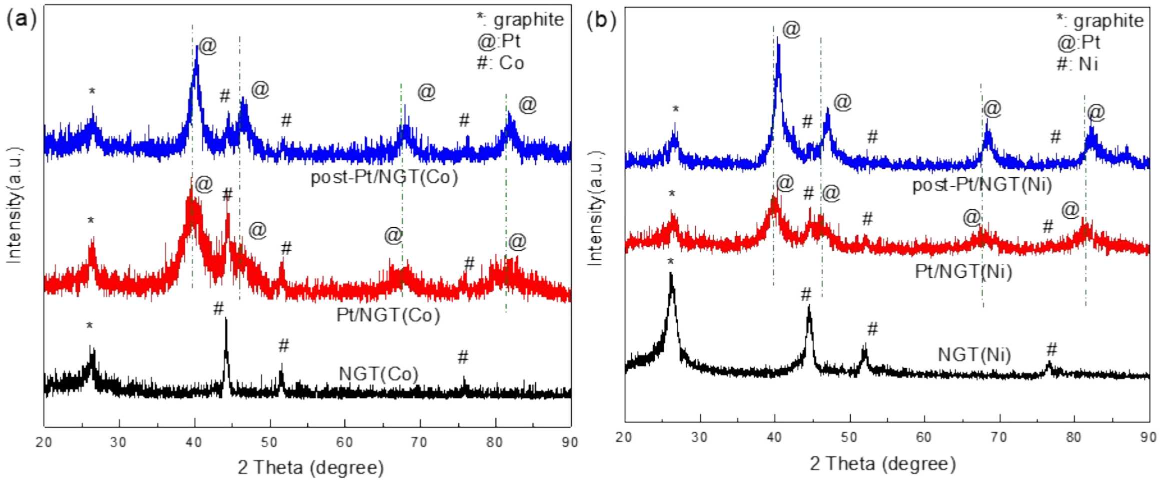

Figure S9. XRD spectra of (a) Co-derived NGT or catalysts and (b) Ni-derived NGT or catalysts.

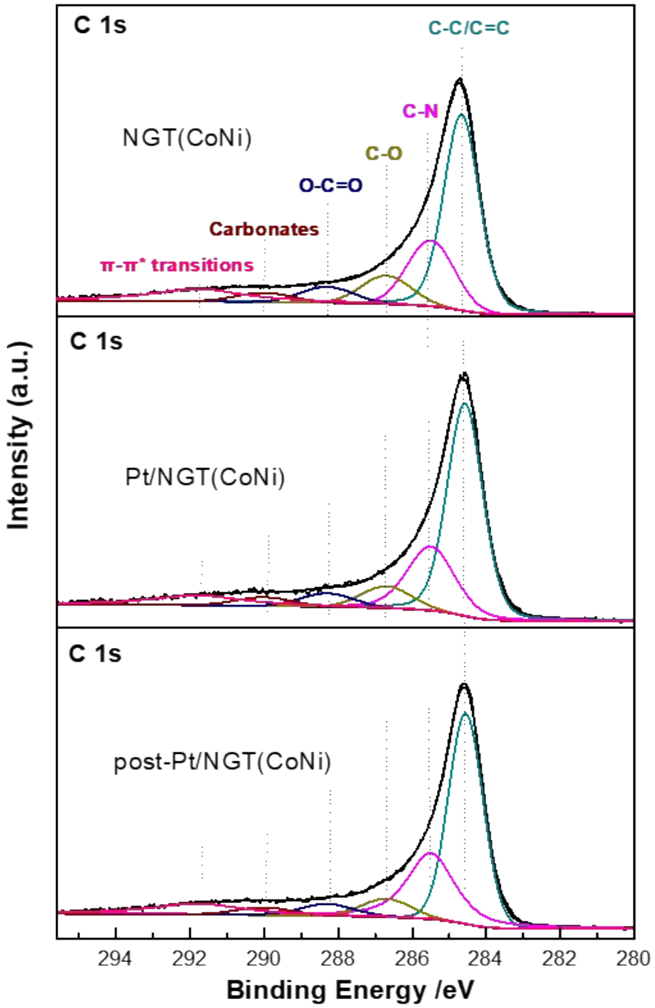

Figure S10. High resolution C 1s XPS spectra of NGT(CoNi), Pt/NGT(CoNi), and post-Pt/NGT(CoNi).

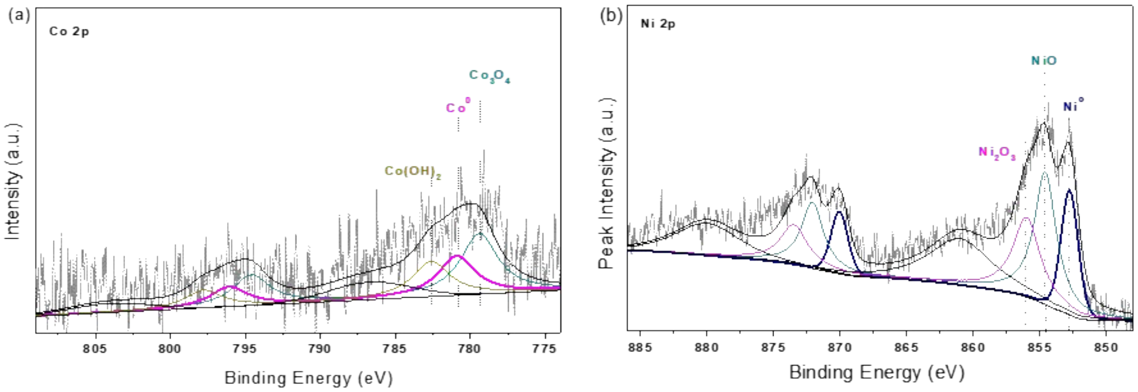

Figure S11. High resolution (a) Co 2p and (b) Ni 2p XPS spectra of post-Pt/NGT(CoNi).

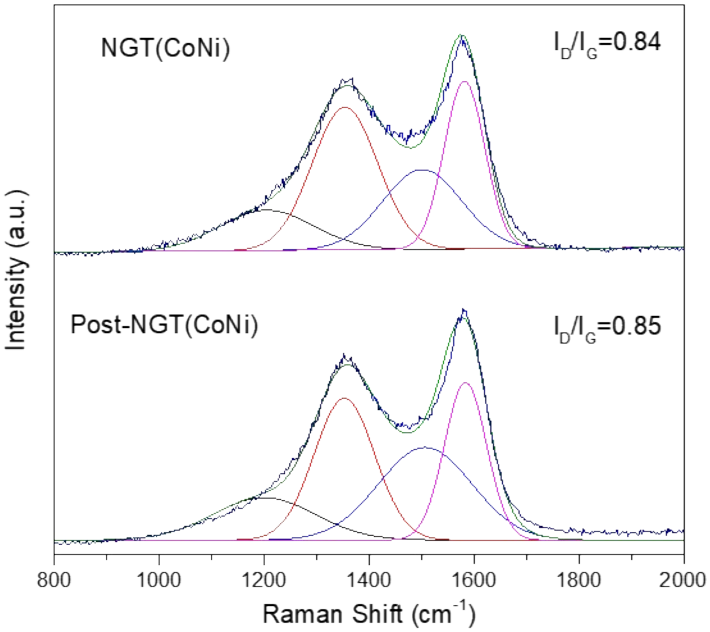

Figure S12. Raman spectra of post-NGT(CoNi) and post-Pt/NGT(CoNi).

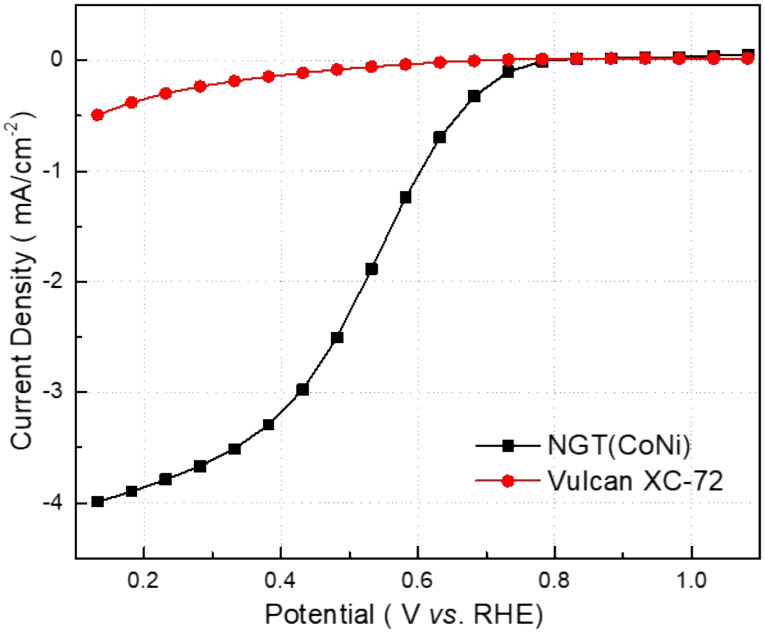

Figure S13. Steady-state polarization plots for NGT(CoNi) and Vulcan XC-72 in 0.1 M $HClO_4$.

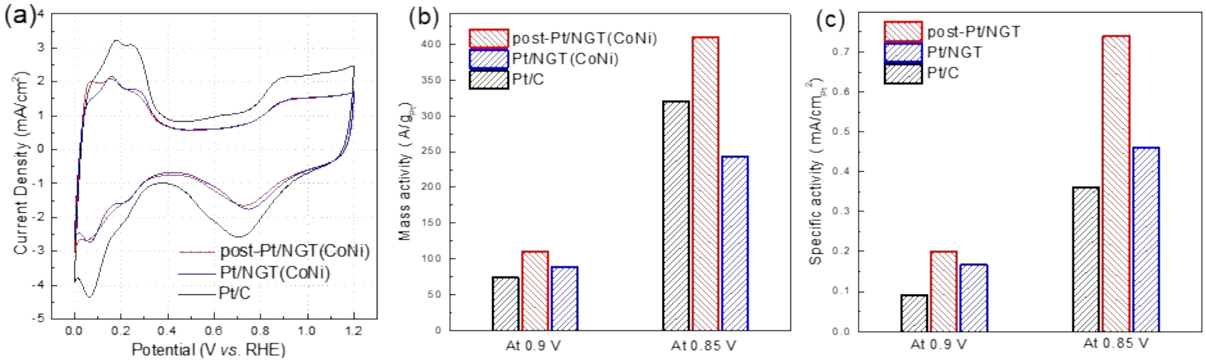

Figure S14. (a) cyclic voltammetry recorded in N_2 for commericial Pt/C, Pt/NGT(CoNi), and post-Pt/NGT(CoNi) in N_2-saturated 0.1 M $HClO_4$ at room temperature. (b) Comparison of mass activities for commericial Pt/C, Pt/NGT(CoNi), and post-Pt/NGT(CoNi) at 0.85 and 0.9 V. (d) Comparison of specific activities for commericial Pt/C, Pt/NGT(CoNi), and post-Pt/NGT(CoNi) at 0.85 and 0.9 V.

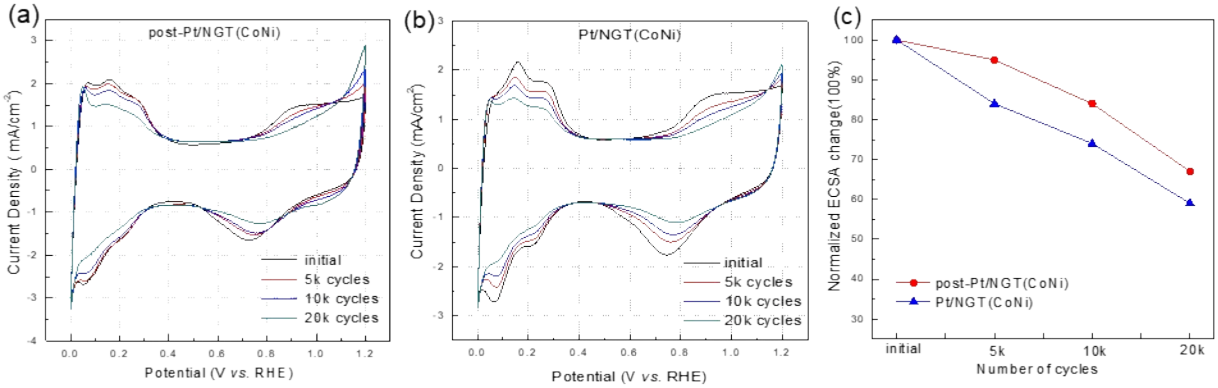

Figure S15. Cyclic voltammetry plots for (a) Pt/NGT(CoNi) and (b)post-Pt/NGT(CoNi) during AST test. Potential cycling range from 0.6 to 1.0 V at a scan rate of 100 mV/s in 0.1 M $HClO_4$ at room temperature. (c) Corresponding normalized ECSA plot as a function of the AST cycling numbers.

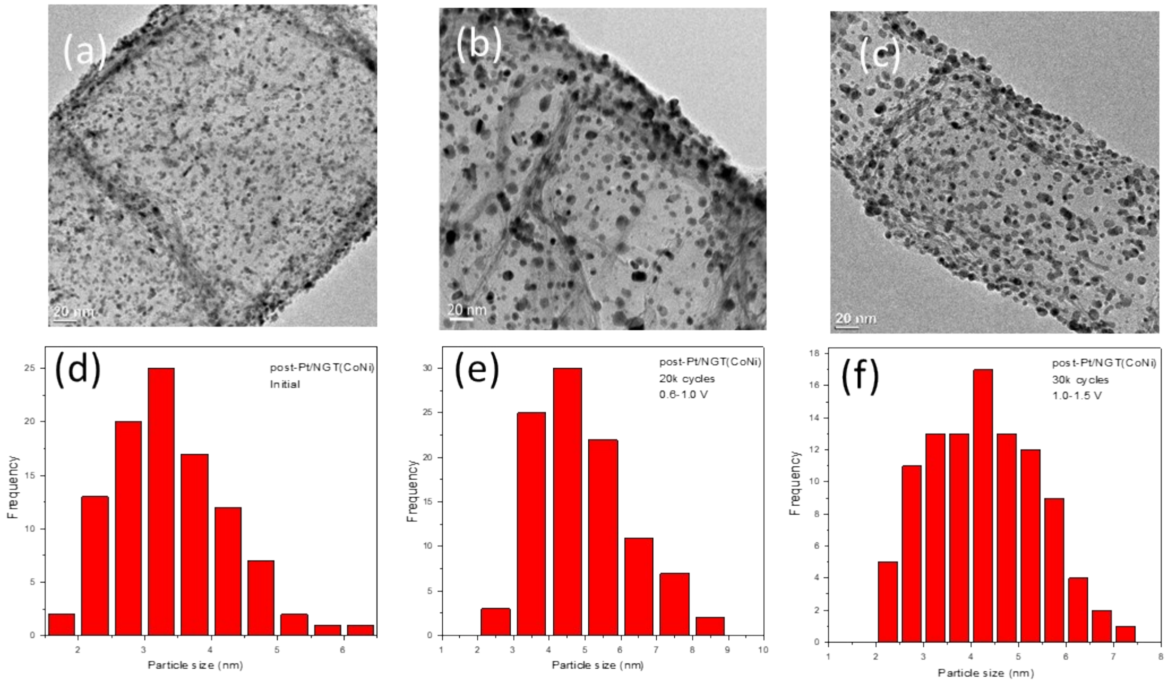

Figure S16. TEM images of (a) fresh post-Pt/NGT(CoNi), (b)post-Pt/NGT(CoNi) after 20k cycles from 0.6-1.0 V vs RHE, and (c) post-Pt/NGT(CoNi) after 30k cycles from 1.0-1.5 V vs RHE. Particle size distribution of (d) fresh post-Pt/NGT(CoNi), (e)post-Pt/NGT(CoNi) after 20k cycles from 0.6-1.0 V vs. RHE, and (f) post-Pt/NGT(CoNi) after 30k cycles from 1.0-1.5 V vs RHE.

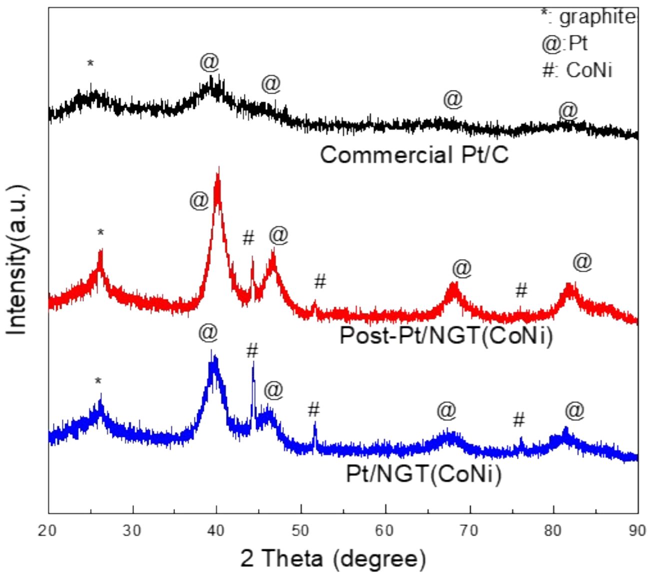

Figure S17. XRD spectra of different Pt cathode catalysts.

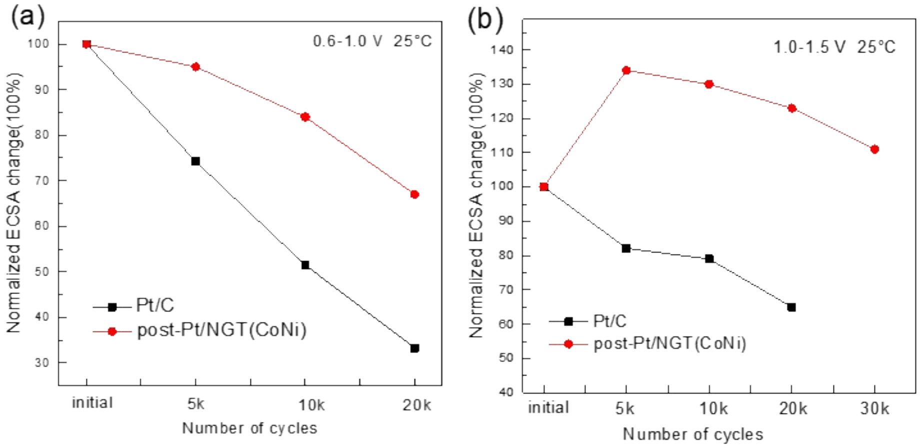

Figure S18. Comparison of normalized ECSA plot as a function of the AST cycling numbers between commercial Pt/C and post-Pt/NGT(CoNi).

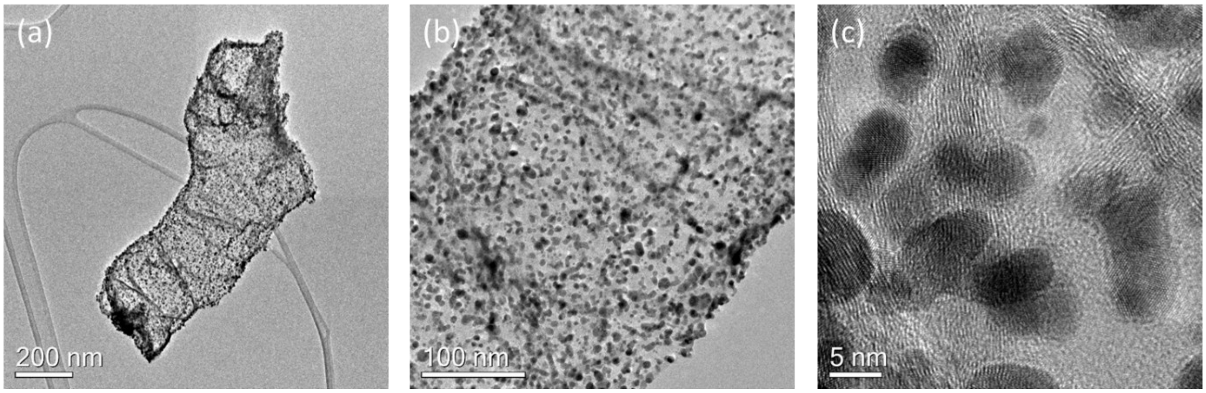

Figure S19. TEM images (a, b) and HR-TEM image (c) of post-Pt/NGT(CoNi) after 10,000 cycles from 1.0-1.5 V vs RHE at 60 °C.

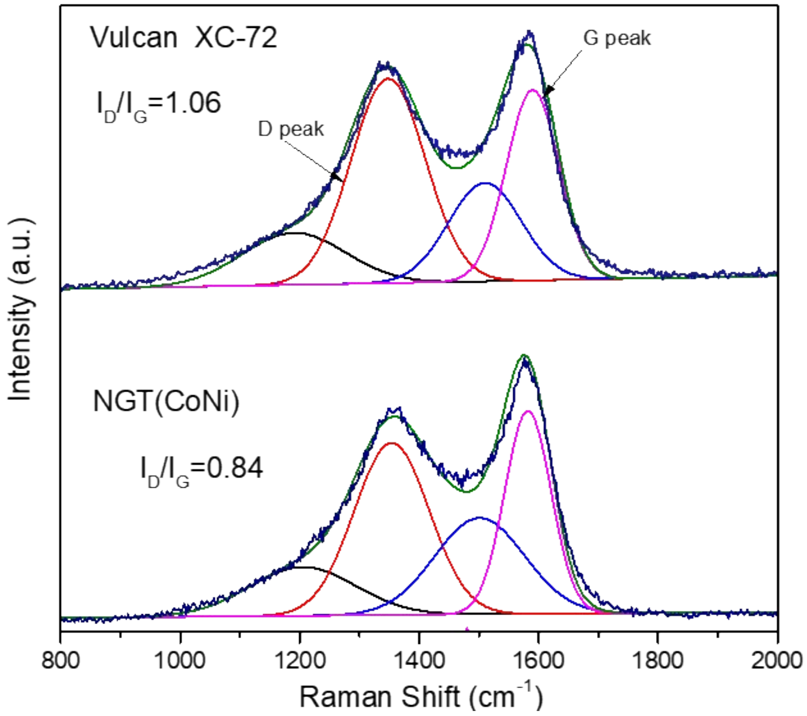

Figure S20. Raman patterns of Vulcan XC-72 and NGT(CoNi) supports.